

# Delivering quantum dot-peptide bioconjugates to the cellular cytosol: escaping from the endolysosomal system†

James B. Delehanty,<sup>\*a</sup> Christopher E. Bradburne,<sup>a</sup> Kelly Boeneman,<sup>a</sup> Kimihiro Susumu,<sup>b</sup> Dorothy Farrell,<sup>b</sup> Bing C. Mei,<sup>‡b</sup> Juan B. Blanco-Canosa,<sup>c</sup> G. Dawson,<sup>d</sup> Philip E. Dawson,<sup>c</sup> Hedi Mattoussi,<sup>b</sup> and Igor L. Medintz<sup>\*a</sup>

Received 20th January 2010, Accepted 10th March 2010

First published as an Advance Article on the web 4th May 2010

DOI: 10.1039/c0ib00002g

For luminescent quantum dots (QDs) to realize their full potential as intracellular labeling, imaging and sensing reagents, robust noninvasive methods for their delivery to the cellular cytosol must be developed. Our aim in this study was to explore a range of methods aimed at delivering QDs to the cytosol. We have previously shown that QDs functionalized with a polyarginine ‘Tat’ cell-penetrating peptide (CPP) could be specifically delivered to cells *via* endocytic uptake with no adverse effects on cellular proliferation. We began by assessing the long-term intracellular fate and stability of these QD-peptide conjugates. We found that the QDs remained sequestered within acidic endolysosomal vesicles for at least three days after initial uptake while the CPP appeared to remain stably associated with the QD throughout this time. We next explored techniques designed to either actively deliver QDs directly to the cytosol or to combine endocytosis with subsequent endosomal escape to the cytosol in several eukaryotic cell lines. Active delivery methods such as electroporation and nucleofection delivered only modest amounts of QDs to the cytosol as aggregates. Delivery of QDs using a variety of transfection polymers also resulted in primarily endosomal sequestration of QDs. However, in one case the commercial PULSin™ reagent did facilitate a modest cytosolic dispersal of QDs, but only after several days in culture and with significant polymer-induced cytotoxicity. Finally, we demonstrated that an amphiphilic peptide designed to mediate cell penetration and vesicle membrane interactions could mediate rapid QD uptake by endocytosis followed by a slower efficient endosomal release which peaked at 48 h after initial delivery. Importantly, this QD-peptide bioconjugate elicited minimal cytotoxicity in the cell lines tested.

<sup>a</sup> Center for BioMolecular Science and Engineering, Code 6900, U.S. Naval Research Laboratory, Washington, DC 20375, USA.  
E-mail: James.delehanty@nrl.navy.mil, Igor.medintz@nrl.navy.mil

<sup>b</sup> Optical Sciences Division, Code 5611, U.S. Naval Research Laboratory, Washington, DC 20375, USA

<sup>c</sup> Departments of Cell Biology & Chemistry, The Scripps Research Institute, La Jolla, CA 92037, USA

<sup>d</sup> Department of Biochemistry and Molecular Biology, University of Chicago, Chicago, IL 60637, USA

† Electronic supplementary information (ESI) available: Additional information detailing the intracellular fate of QDs, attempted endosomal release and control experiments for the intracellular stability of the polyhistidine-QD association. See DOI: 10.1039/c0ib00002g

‡ Current address: Avon Products, Inc., One Avon Place, Suffern, NY 10901, USA.

§ Current address: Florida State University, Department of Chemistry and Biochemistry, Tallahassee, FL 23306, USA.

## Introduction

The unique spectral properties of luminescent semiconductor nanocrystals or quantum dots (QDs) have established them as attractive reagents for the long-term visualization of cellular structures and processes.<sup>1–4</sup> As a result, considerable effort has been invested in recent years in the development of facile yet robust methods for the specific cellular delivery of QDs, with a particular emphasis on achieving delivery to the cytosol.<sup>5–10</sup> The methods employed to date for the intracellular delivery of QDs can be grouped into three generalized categories based on their physicochemical nature. Passive delivery is a nonspecific process that relies on the inherent physicochemical properties of the QD (surface charge and/or functionalization) to

### Insight, innovation, integration

Nanoparticle-mediated drug delivery is a burgeoning field at the intersection of materials, biology and medicine that seeks to overcome many of the issues associated with systemically delivered therapies. Key to its success will be the ability to mediate the facile delivery of nanoparticle materials to the cytosol of mammalian cells. Herein, we extensively evaluate available methods for achieving the

reliable and timely delivery of quantum dots to the cytoplasm of cells and find that a multifunctional peptide may be able to accomplish this. It is envisioned that similar delivery regimes which specifically exploit cell-targeting technologies will significantly further the use of bio-functionalized nanoparticles as vehicles for targeted therapeutic drug delivery.

mediate uptake. Facilitated delivery utilizes a delivery agent (*e.g.*, cationic peptide or polymer) that is covalently attached to or electrostatically complexed with the QDs to specifically induce internalization. Both these techniques, while non-invasive, typically utilize the endocytic pathway which results in encapsulation of the QDs within intracellular endolysosomal vesicles and thus requires further strategies to liberate the sequestered QDs to the cytosol if that is ultimately desired.<sup>6,11,12</sup> Examples of the latter include using additional chemicals such as sucrose or chloroquine or adding polymers such as polyethyleneimine during delivery to disrupt the endosomes by osmotic shock. Lastly, active delivery methods such as electroporation and microinjection deliver QDs directly to the cytosol through physical manipulation of the cell. However, these are highly invasive techniques that can often compromise the integrity of cellular structures and substantially reduce cellular viability.<sup>10</sup>

We have previously demonstrated that efficient cellular uptake of CdSe–ZnS core–shell QDs could be mediated by a polyarginine-bearing cell-penetrating peptide (CPP) derived from the HIV-1 Tat protein.<sup>13</sup> The peptide was self-assembled onto the QD surface *via* non-covalent metal-affinity interactions between a polyhistidine domain (His<sub>n</sub>), appended at the peptide's N-terminus and the Zn-atoms on the QD surface.<sup>14</sup> This assembly process is rapid and facile and the conjugates could be incubated with cells within minutes of QD-peptide mixing. A one hour incubation with both HEK 293T/17 and COS-1 cells was sufficient to mediate specific uptake; the degree of which was found to be dependent on both QD concentration and peptide valence (*i.e.* the number of peptides assembled onto the QD). This strategy also allowed CPP-functionalized QDs to undergo specific uptake even in the presence of other unlabeled QD species in the culture media. Counterstaining with the endosomal marker protein transferrin showed that in all cases the QDs were sequestered within endocytic vesicles. It is generally accepted that the CPP's positively-charged polyarginine domain mediates initial electrostatic interactions of the QD–CPP complexes with negatively charged cell surface receptors (*e.g.*, heparan sulfate proteoglycans) that undergo constitutive endocytosis.<sup>15</sup> We also found that cytotoxicity following QD delivery was a direct function of cellular exposure time and QD concentration. Upon one hour incubation, sufficient time to achieve adequate cellular uptake and labeling, no significant change in cellular proliferation was observed in two cell lines tested. Incubation of the QD-complexes for 24 h or longer, however, led to dose-dependent cytotoxic effects. We have further demonstrated that the same CPP could mediate the specific cellular uptake of QDs conjugated with yellow fluorescent protein or b-phycoerythrin light harvesting complexes.<sup>16</sup> For the latter, the molecular weight of protein cargo arrayed around each QD on average surpassed 1000 kDa.

Here, we continue from those initial studies and investigate the intracellular fate of the QD–CPP complexes by counterstaining various intracellular compartments. We found that the internalized QD–CPP conjugates remained sequestered as intact complexes within endolysosomal vesicles over the course of three days in culture. As our ultimate goal was the cytosolic delivery of QDs, we extensively tested various uptake

methods to identify viable strategies capable of cytosolic QD delivery to large numbers of cells. We found that active techniques such as electroporation and nucleofection delivered only modest amounts of aggregated QDs to the cytosol. Facilitated delivery methods employing cationic amphiphiles, polymers or peptides (see Fig. 1) also resulted in endosomal QD sequestration. The commercial amphiphilic PULSin™ polymer did, however, mediate a modest degree of QD endosomal release but only after four days and with considerable cytotoxicity. Lastly, we found that an amphiphilic peptide could mediate both rapid endocytic uptake of QDs followed by a slower endosomal release over 48 h with minimal concomitant cytotoxicity. Our results are discussed within the context of ongoing efforts to identify facile means by which to achieve cytosolic QD delivery.

## Results and discussion

### QD materials and delivery agents

Representative absorption and emission spectra of the QD materials used in this study are shown in Fig. 1A. A schematic representation of the QDs and the various delivery agents used to self-assemble to the QD surface are depicted in Fig. 1B.

### Long-term intracellular fate of QD–CPP conjugates

We began by following the intracellular fate of the delivered QD–CPP complexes at time points longer than 1 h in cell culture. We incubated HEK 293T/17 cells with DHLA-capped 510 nm-emitting QDs complexed with the CPP while counter-labeling the endosomes (AlexaFluor 647-transferrin), lysosomes (LysoTracker Red DND-99), or the Golgi complex (BODIPY TR-ceramide-BSA). Numerous previous studies have demonstrated and confirmed the utility of these commercially available probes for the time-resolved labeling of these various subcellular compartments.<sup>17–20</sup> As shown in Fig. 2A, at 1 h post-delivery the QDs adopted a punctate, vesicular appearance with QD fluorescence in green overlapping the endosome and lysosome markers, while no overlapping QD signal was observed with the Golgi complex markers. This confirms that the QD–CPP complexes were located within the endolysosomal system in agreement with our previous results.<sup>13</sup> Similar data was collected for cells exposed to QD–CPP complexes and the same markers at 4, 24 and 72 h after delivery (see Fig. 2B). After 3 d, the QD–CPP complexes still colocalized with the endolysosomal markers although we noted that at the later time points, the QD distribution appeared to be primarily perinuclear reflecting their location within more mature endosomes. When the cells were cultured beyond 3 d, similar results were obtained (data not shown). This demonstrates that while the CPP mediates the efficient uptake of the QDs, it does not facilitate the release of the QDs to the cytosol over time. Similar data were obtained with DHLA–PEG capped QDs showing that the nature of the capping ligand, *i.e.*, charged *vs.* neutral, also had no effect on intracellular QD fate over time (see Supporting Information, Fig. S1†).

The endolysosomal fate of the CPP-delivered QDs is in good agreement with results reported by other groups.

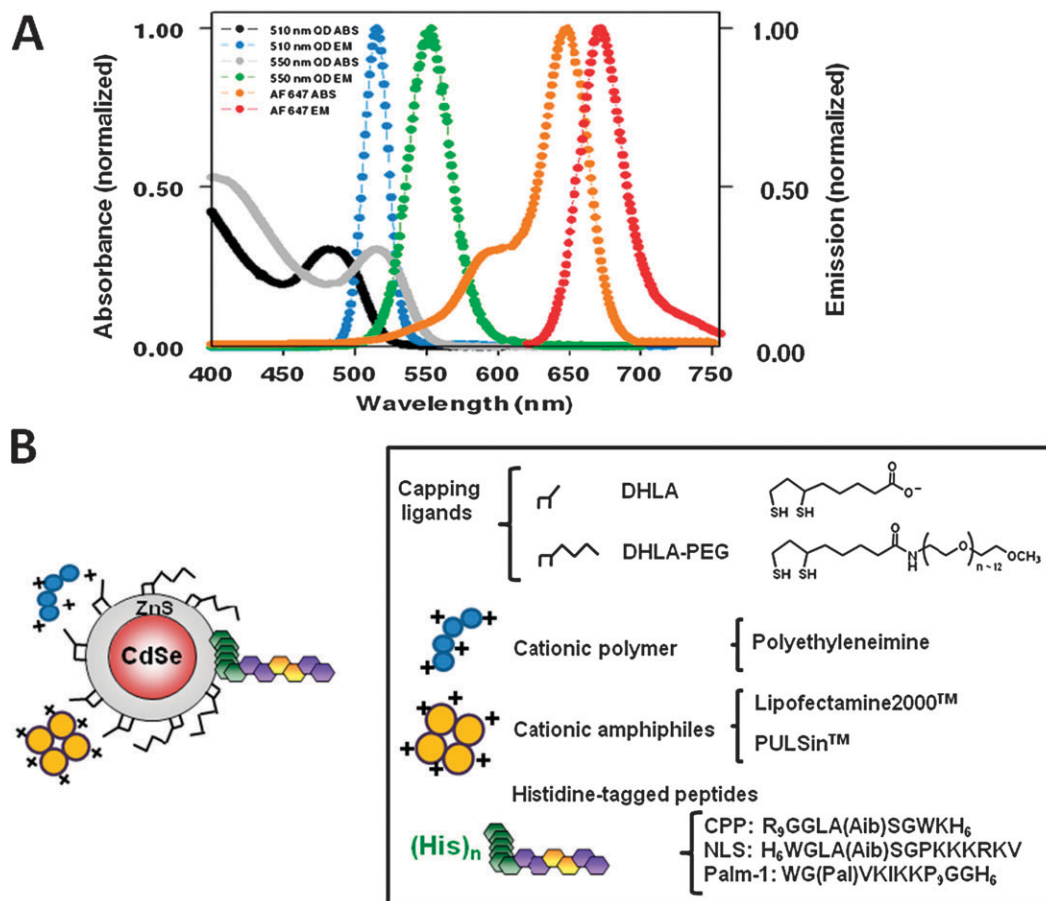


**Fig. 1** Spectral properties and schematic of QD conjugates used in this study. (A) Normalized absorbance and emission of 510, 550 nm QDs and AlexaFluor 647 (AF647). (B) Schematic of QD conjugates for facilitated QD delivery. CdSe–ZnS core–shell QDs capped with either charged DHLA or neutral DHLA–PEG ligands are noncovalently associated with linear cationic polymers, cationic liposomes or histidine-tagged peptides to mediate QD endocytosis. The sequences of the CPP, NLS and Palm-1 peptides used in this study are shown. (Aib, alpha-amino isobutyric acid; *Pal*, palmitate).

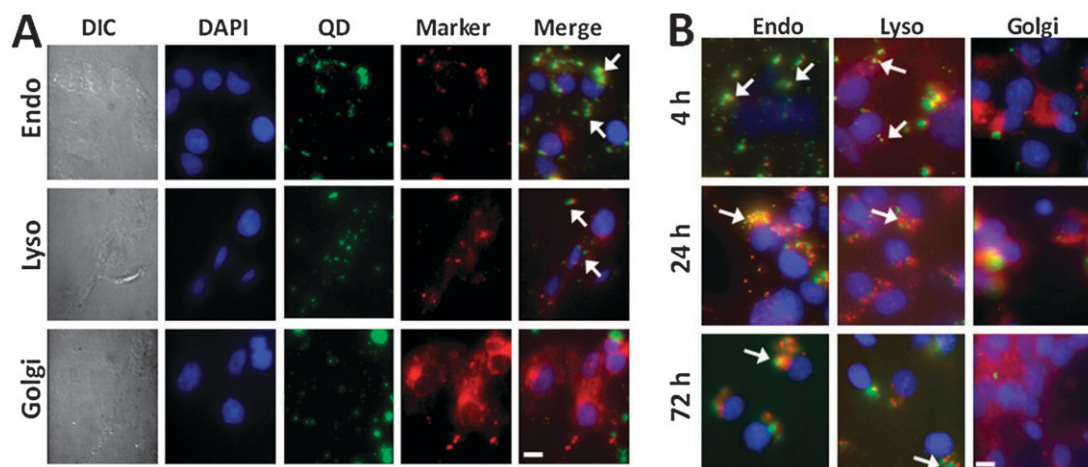


**Fig. 2** QD–CPP internalization and colocalization over time. HEK 293T/17 cells were incubated with 510 nm DHLA–QDs appended with CPP (QD: CPP ratio 1:25) at a QD concentration of 60 nM for 1 h. Fluorescent markers for counterstaining the endosomes, lysosomes and Golgi complex were included as described. After 1 h, the cells were washed, fixed and stained with DAPI (A) or supplied with fresh media and cultured for 4, 24 or 72 h prior to fixation and DAPI-staining (B). In panel (A) the DAPI, QD and marker signals are shown individually and merged while in panel (B) only the merged images are shown. Arrows indicate areas of colocalization. Scale bar is 10  $\mu$ m.

Tekle *et al.* found that commercial streptavidin-conjugated QDs decorated with various biotinylated delivery ligands including the plant toxin ricin, Shiga toxin, or transferrin remained sequestered within the endocytic vesicles of HeLa cells after uptake and did not recycle to other intracellular trafficking compartments.<sup>21</sup> They also noted that approximately 3–4 h following delivery, the QDs had also accumulated in what appeared to be more perinuclear endosomes. In the absence of QDs, fluorescently-labeled ricin and Shiga toxins were routed to the Golgi apparatus as expected. Ruan and co-workers also monitored the intracellular trafficking of streptavidin-conjugated QDs assembled with biotinylated Tat peptides in HeLa cells.<sup>12</sup> They showed that the endosome-encapsulated QD-peptide complexes were associated with the inner leaflet of the vesicle membrane and were actively transported to an asymmetric perinuclear region known as the microtubule organizing center (MTOC). Accumulating data suggests that endosomal entrapment of QDs appears to occur regardless of the size of the associated ligand used to mediate uptake.<sup>10</sup> For example, QDs delivered with disparate functional ligands ranging in size from small molecules (folate, 450 Mw),<sup>22</sup> to peptides (Tat, <5000 Mw), small proteins (Cholera toxin B, 12 000 Mw) and even large proteins such as antibodies (150 000 Mw)<sup>23</sup> were all found in endosomes. Collectively, these findings demonstrate the importance of confirming the intracellular fate of nanoparticles and illustrate the need for the development of methods that facilitate cytosolic delivery of QDs.

### Intracellular stability of QD–CPP assemblies

A chief requirement for the successful implementation of QD-peptide and QD-protein conjugates in intracellular delivery applications is their long-term stability during uptake as well as once they are inside the cell. For example, labeling specific subcellular organelles such as mitochondria or the nucleus with QD-peptide conjugates requires the stable association of the targeting peptide with the QD surface throughout the uptake and targeting process. Of particular interest in the case of our self-assembled QD–CPP (generated by polyhistidine–zinc interactions) is the conjugate stability within the endolysosomal vesicles during the three day culture period. Given that the normal  $pK_a$  of histidine residues is  $\sim 6.5$  and that the pH of the vesicles can drop to as low as  $\sim 5.0$  to  $5.5$  during the formation of late endosomes and lysosomes,<sup>24</sup> protonation of the imidazole side chains of the polyhistidine tract could result in dissociation of the CPP from the QD surface. Alternatively, several proteases including cathepsins along with several aspartate proteases are endogenously expressed in the endolysosomal system and these may also proteolyze the peptides.<sup>25</sup> Thus, confirmation of the long-term intracellular stability of our QD–CPP assemblies was warranted.

To investigate this issue, we self-assembled QD-peptide conjugates that engaged in FRET and monitored their intracellular photophysical interactions over time. 510 nm DHLA-capped QDs were first assembled with an average of  $\sim 2$  Cy3-labeled His<sub>6</sub>-peptides and then the CPP was added to form the full conjugate (schematic in Fig. 3A). Due to the

peptide's small size and proximity of the Cy3 acceptor to the nanocrystal surface, this valence results in a *ca.* 40% quenching of the QD photoluminescence (PL) by FRET (data not shown). The resulting conjugates were delivered to HEK 293T/17 cells and the cells were cultured for three days. QD-donor and Cy3-acceptor FRET interactions over time within the cells were measured by exciting the QD and collecting side-by-side split fluorescence images using a DualView system and deconvoluting the subsequent intensity data, see Experimental. The excellent spectral separation ( $\sim 60$  nm) between the QDs and Cy3 emission maxima facilitated this collection. Fig. 3B shows representative images in which the QD and Cy3 signals are merged at various time points during the culture period. A distinct one-to-one overlap in the punctate signals of both QD and dye was observed demonstrating colocalization of the QDs and Cy3-labeled peptides within endocytic vesicles throughout the culture period. Analyses of the signals showed the pair was actively engaged in FRET (close proximity) and not just present within the same endosomal compartments. When the Cy3/QD emission ratio (normalized and corrected for direct Cy3-acceptor excitation) was calculated, a gradual decrease was observed over time, culminating in a 36% decrease over three days (Fig. 3C). A decrease in this ratio would result from either Cy3-peptide dissociation from the QD surface (loss of His<sub>6</sub> interactions or proteolysis) or by chemical degradation of the dye. Thus, control experiments were performed to determine the extent of degradation of the Cy3 dye. When Cy3 was delivered to the endosomes as a Cy3-labeled transferrin conjugate (no QDs present), the fluorescence output of the dye decreased approximately 34% over the same time period, in excellent agreement with the decrease observed in the above QD–CPP–Cy3-labeled peptide constructs (Fig. 3D and Supporting Information Fig. S2<sup>†</sup>). Control experiments performed with QD donors alone showed no change in the relative QD PL (data not shown). These results suggest that the His<sub>6</sub>-bearing peptides remain stably conjugated to the QD Zn-surface, even within the acidic environment of the endocytic vesicles over time. We attribute this strong affinity, even at lower pH, to cooperative interactions resulting from the multiple histidine residues present on each peptide interacting with the QD surface.<sup>14</sup> Prior to this report, the stability of the QD-peptide conjugates within endosomes had only been verified for one hour after uptake using two-photon excitation FRET microscopy.<sup>26</sup> Thus, our results presented herein represent the first instance in which the His–zinc interaction has been shown to be stable *intracellularly* over three days. This finding has important implications for the use of this QD conjugate assembly strategy in long-term intracellular labeling and imaging applications.

### Cytosolic delivery of QDs

Having confirmed the long-term sequestration of QDs within endosomes following CPP-facilitated uptake, our next objective was to identify a means by which to deliver QDs to the cytosol. We thus undertook an exhaustive investigation of methodologies to either: 1-deliver the QDs directly to the cytosol *via* direct physical manipulation of the cell

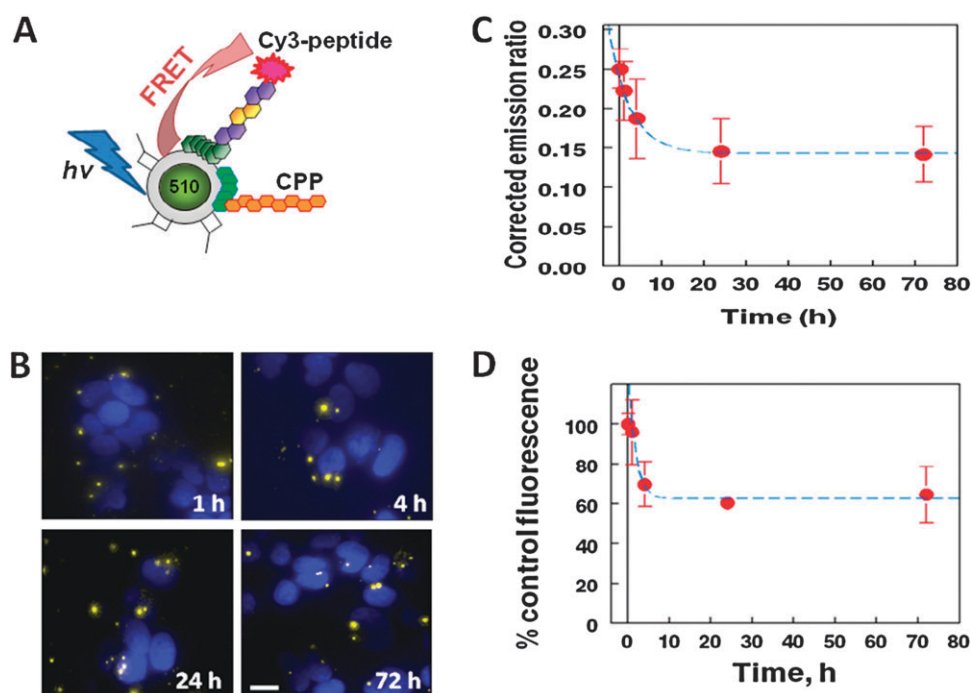


**Fig. 3** Intracellular stability of polyhistidine-QD association. (A) 510 nm DHLA QDs were appended with 25 CPP to mediate uptake in HEK 293T/17 cells and  $\sim 2$  Cy3-labeled peptides to monitor the FRET between the QD and the Cy3 dye over time (figure not to scale). (B) Merged images of DAPI-stained nuclei, QD and Cy3 signals at 1, 4, 24 and 72 h after conjugate delivery. Scale bar is 10  $\mu\text{m}$ . (C) The calculated Cy3/QD emission ratio is shown plotted as a function of time after initial conjugate delivery. (D) The observed fluorescence for transferrin-Cy3 conjugates delivered alone (no QDs) is plotted as a function of time. (Images of cell-internalized transferrin-Cy3 conjugates over this time course are shown in Supporting Information Fig. S2†). In (C) and (D) the data points were fitted with a dose response logistic curve fit function.

(active delivery) or 2-decorate the QDs with peptides or polymers that could mediate both endocytic uptake and the subsequent release of the QDs from within endocytic vesicles (facilitated delivery followed by endosomal escape). The individual approaches are summarized in Table 1 and the results of the various methods tested are discussed in the following sections.

**Active delivery.** Electroporation and nucleofection are primarily used for the cellular delivery of nucleic acids and employ an externally applied electric field to increase the excitability and permeability of the membrane's phospholipid bilayer allowing the intrinsically charged extracellular materials to directly enter the cytosol during an electric pulse.<sup>27</sup> Nucleofection further incorporates a proprietary transfection reagent to mediate the subsequent localization of internalized materials to the nucleus.<sup>28,29</sup> As shown in Fig. 4A and B, when 550 nm DHLA-PEG capped QDs were delivered to HEK 293T/17 cells using electroporation or nucleofection, they adopted a punctate morphology indicative of QD aggregation within the cytosol. This delivery bypassed the endosomes as confirmed by transferrin counterstaining (data not shown). In contrast, when QDs capped with these same ligands were microinjected into cells, they adopted a highly disperse staining across the entire cytosol for long periods of time.<sup>30</sup> This indicates that the electric field and/or process itself adversely affects subsequent intracellular QD solubility. Further, no evidence of nuclear accumulation or localization within the perinuclear spaces was observed even

after extended culture following delivery for both methods. We also noted a high degree of cell death and estimate that only 50% of cells remained viable following delivery attempts.

Electroporation-based QD delivery has yielded similar results in previous reports. Derfus *et al.*, reported intracellular aggregation of PEG-coated commercial CdSe-ZnS QDs delivered to HeLa cells *via* electroporation.<sup>31</sup> These appeared to also be located outside the endosomes. Chen and Gerion electroporated HeLa cells with streptavidin-conjugated silanized QDs preassembled with biotinylated nuclear localization peptides.<sup>32</sup> While they also observed a large degree of QD aggregation, they were able to confirm the accumulation of a small portion of the QDs within the nucleus and perinuclear spaces. Their results indicate that perhaps not all of the delivered QDs completely precipitated intracellularly following electroporation and that this may be dependent upon the nature of the surface coating materials. Cumulatively, the QD aggregation and subsequent high cellular morbidity suggest that electroporation and nucleofection are not effective means of delivery despite their ability to access QDs directly to the cytosol.

**Facilitated delivery.** Facilitated delivery of QDs involves the use of exogenous agents that are added to the extracellular medium or complexed with the QDs to exploit the cell's innate processes of pinocytosis or endocytosis. Pinocytosis, or fluid-phase uptake, is a nonspecific form of endocytosis in which minute amounts of extracellular fluids and materials are internalized within small vesicles. Endocytosis, in contrast, is



**Table 1** Summary of QD delivery strategies used in this study

Delivery method/agent	Mechanism of uptake	Quantum dot fate and toxicity
<b>Active delivery</b>		
Electroporation	Membrane pore formation	Poor uptake, QDs aggregated, toxic <sup>a</sup>
Nucleofection	Membrane pore formation	Poor uptake, QDs aggregated, toxic <sup>a</sup>
<b>Facilitated delivery</b>		
<i>Pinocytosis</i>		
Influx™	Pinocytosis	Endosomal, QDs punctate, moderately toxic <sup>a</sup>
<i>Polymer-mediated</i>		
Lipofectamine2000™	Endocytosis	Endosomal, QDs punctate, toxic <sup>b</sup>
Polyethyleneimine	Endocytosis	Endosomal, QDs punctate, toxic <sup>a</sup>
PULSin™	Endocytosis	Cytosolic, QDs dispersed, toxic <sup>b</sup>
<i>Peptide-mediated</i>		
CPP peptide	Endocytosis	Endosomal, QDs punctate, minimally toxic <sup>b,c</sup>
NLS peptide	Endocytosis	Endosomal, QDs punctate, minimally toxic <sup>b</sup>
Palmitoylated peptide (Palm-1)	Endocytosis	Cytosolic, QDs dispersed, minimally toxic <sup>b</sup>
<i>Augmented peptide-mediated</i>		
CPP peptide + sucrose	Endocytosis	Cytosolic, QDs punctate, toxic <sup>a</sup>
CPP peptide + chloroquine	Endocytosis	Cytosolic, QDs punctate, toxic <sup>a</sup>
CPP peptide + pyrenebutyrate	Membrane translocation	Mixed membranous and endosomal, toxic <sup>a</sup>

<sup>a</sup> General toxicity assessment made by visual inspection of cellular morphology and rate of proliferation compared to control cells during delivery experiments. <sup>b</sup> Toxicity measured by cell proliferation assay as described in the Experimental. <sup>c</sup> Toxicity reported in ref. 13.

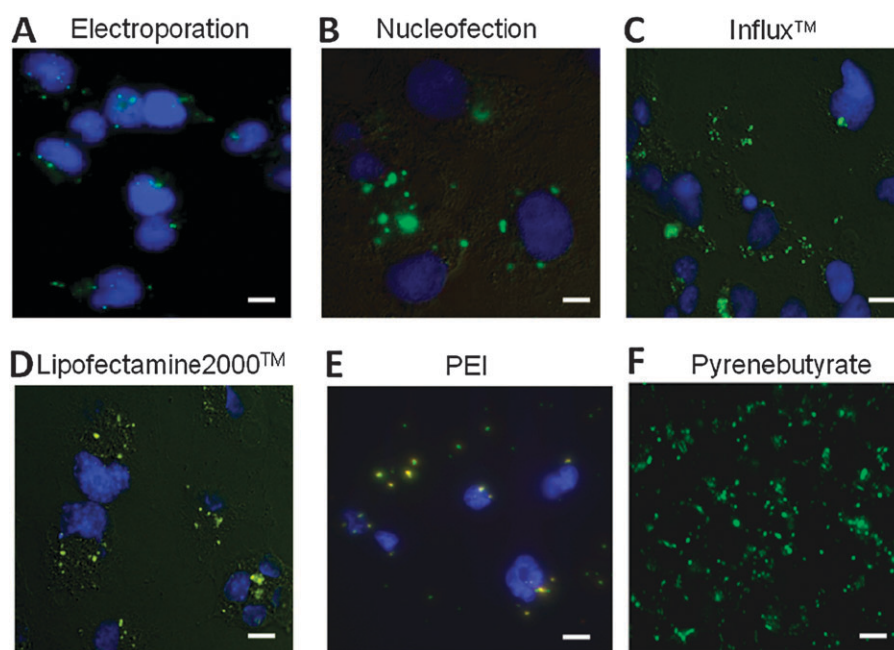


**Fig. 4** Cellular delivery of QDs using various active and facilitated methods. 510 nm DHLA-PEG QDs at a concentration of 400–500 nM were delivered to HEK 293T/17 cells by electroporation (A) or nucleofection (B). In both instances, the delivered QDs form intracellular aggregates. (C) 510 nm DHLA-PEG QDs (800 nM) were delivered using the pinocytic reagent, Influx™. QDs are punctate, indicative of sequestration within pinocytic vesicles. 520 nm QDs (75 nM) capped with a 1 : 1 mixed surface of DHLA:DHLA-PEG were delivered to HEK 293T/17 cells using Lipofectamine2000™ (D) or the branched polymer, polyethyleneimine (E). The images in (D) and (E) show merged images of the QD signal and the fluorescence from the endocytic marker, AlexaFluor 647-transferrin. The QDs appear punctate and are colocalized with transferrin (note yellow color of the merged QD and transferrin signals). In (A) through (E) the cells were imaged after fixation and staining with DAPI (blue). (F) 550 nm DHLA-PEG QDs (100 nM) appended with 25 CPP were coincubated with 100 μM pyrenebutyrate in PBS for 30 min at 37 °C prior to washing and imaging of live cells (no DAPI present). The QDs appear punctate, indicative of endosomal sequestration. Scale bar is 10 μm.

a specific process as the uptake of extracellular materials is mediated by their interaction with cognate cell surface receptors that become spatially concentrated within the

forming endocytic transport vesicles.<sup>33,34</sup> The exogenous agents for facilitated delivery can take the form of chemicals or drugs that are co-incubated with the QDs during the

delivery process or alternatively they can be polymers or peptides that are either covalently attached or non-covalently associated (electrostatically) with the QD surface.

**Pinocytosis-mediated delivery.** To exploit this process, we utilized the commercial pinocytosis reagent known as Influx™. This reagent is co-incubated with the QDs and cells in a hypertonic medium which promotes the uptake of extracellular materials within pinocytotic vesicles. The cells are then briefly incubated in a hypotonic medium to swell and disrupt the vesicles, releasing the internalized materials into the cytosol; in essence this is a modified intracellular osmotic shock protocol. A solution of 510 nm DHLA-PEG QDs was prepared in the hypertonic delivery media (including the Influx™ reagent) and incubated with HEK 293T/17 cells for the recommended period of time for uptake (~30 min). As shown in Fig. 4C, we observed only a modest degree of uptake even when the QD concentration was significantly increased to 800 nM. Further, the intracellular QD morphology remained punctate even after several days, indicating their persistent localization within pinocytotic vesicles. Jaiswal *et al.* reported similar long-term intracellular sequestration of pinocytically delivered QDs.<sup>6</sup> In that study, 400–600 nM negatively charged DHLA-capped CdSe/ZnS QDs were incubated with HeLa cells for 2–3 h without any exogenous pinocytosis reagent present. Using a plasmid-expressed fluorescent protein endosomal marker for counter-labeling, the authors showed that the QDs remained trapped within vesicles for up to nine days in culture.

**Polymer-mediated delivery.** A number of commercial cationic polymers have been developed for gene delivery and transfection applications. These reagents self-assemble electrostatically to negatively-charged species (*e.g.*, nucleic acids) while simultaneously mediating interactions of the resulting complex with the plasma membrane to induce endocytosis. Once compartmentalized within intracellular vesicles, it is believed that the cationic polymers can facilitate endosomal disruption *via* osmotic lysis (the ‘proton sponge’ effect), releasing the vesicle contents to the cytosol.<sup>35,36</sup> We hypothesized that QDs bearing a net negative surface charge could complex with such polymers and thus utilized 520 nm QDs capped with a 1 : 1 mixed surface of DHLA:DHLA-PEG ligands. This cap exchange strategy provides both a charged QD surface moiety (DHLA) along with the extended pH stability provided by the PEG ligands.<sup>30,37</sup> Initial experiments utilized the well-known cationic liposomal transfection reagent Lipofectamine2000™. QD-Lipofectamine complexes were formed as described in the Experimental section and incubated with HEK 293T/17 cells for 4 h. As shown in Fig. 4D, we found that the QDs were completely colocalized with the co-delivered transferrin endosomal marker. Extended monitoring of the cells for several days after delivery did not reveal any changes in this morphology (data not shown). Interestingly, Derfus *et al.* demonstrated that commercial PEG-coated QDs delivered to HeLa cells using this reagent appeared to be largely present within the cytosol.<sup>31</sup> However, their interpretation was complicated by the fact that the QDs also formed aggregates of several hundred nanometres in diameter within the cytosol and were

not well dispersed. It was also not apparent if the liposomal polymer was responsible for inducing the intracellular QD aggregation in that case.

Polyethyleneimine (PEI) is a cationic polymer that is sometimes used as a reagent for transfecting nucleic acids into mammalian cells and has recently been used for cellular uptake of QDs. Duan *et al.* synthesized dendritic PEG-grafted PEI ligand molecules and used them to functionalize CdSe-CdS-ZnS core-shell-shell QDs.<sup>38</sup> They demonstrated that this specific combination of surface chemistries could mediate both endocytosis and subsequent cytosolic delivery of these QDs to HeLa cells. The efficiency of QD endosomal escape could be enhanced by increasing the PEI content in the PEG-PEI ligand. However, the increased PEI content was also coupled with significant cytotoxicity as cellular viability dropped to only 40% with this more efficient endosomal escape capping ligand. We tested the combination of PEG and PEI for cellular uptake by complexing 520 nm QDs capped with 1 : 1 DHLA:DHLA-PEG ligands with increasing ratios of PEI (~0.5–10 µg PEI per 1 pmol QD) and then exposing them to HEK 293T/17 cells for 1–3 h. As demonstrated by the representative micrograph in Fig. 4E, complete colocalization of the QDs with the transferrin marker within endosomes was noted for all concentrations tested even after several days. We similarly noted a considerable degree of cytotoxicity that tracked the increasing concentrations of PEI used to form the QD-PEI complexes (data not shown).

Jablonski *et al.*, recently reported the ability to rapidly deliver polyarginine peptide-bearing QDs directly to the cytosol using an excess of the hydrophobic counterion, pyrenebutyrate.<sup>39</sup> Using streptavidin conjugated QDs assembled with biotinylated polyarginine peptides in the presence of >1000 fold molar excess pyrenebutyrate (4 µM) per QD (4 nM), the authors demonstrated rapid cellular delivery of the QDs (~5 min) to BS-C-1 monkey kidney cells which appeared to be well dispersed within the cytosol. They surmised that the anionic pyrenebutyrate bound to the cationic polyarginine to form a hydrophobic polymeric complex that could pass directly through the plasma membrane. When we incubated HEK 293T/17 cells with 550 nm DHLA-PEG QD-CPP assemblies (100 nM in QDs) in the presence of a far higher concentration of pyrenebutyrate (100 µM), however, the QDs initially remained entirely associated with the plasma membrane even after an ~6× longer incubation of 30 min. After 3 h, the QDs took on a punctate appearance, indicative of endosomal uptake and no cytosolic dispersal was observed (see Fig. 4F and Supporting Information Fig. S3†). It is currently unclear what role pyrenebutyrate plays in the uptake process and these results suggest it is likely that differences in the QD materials (*i.e.* presence or absence of a covalently attached 60 kDa streptavidin protein along with different surface ligands) may actually play a more profound part in determining the nature of the QDs interaction with the plasma membrane.

The last molecule we tested in this class of materials was the commercially available PULSin™, a proprietary amphiphilic polymer originally designed as a cytosolic delivery agent for proteins. We found that PULSin™ could mediate efficient uptake of QDs and a modest subsequent endosomal release

to the cytosol over a much longer time period of 3–4 d. As shown in Fig. 5A and B, PULSin™ complexation resulted in the initial endosomal uptake of 520 nm DHLA:DHLA-PEG QDs to both COS-1 and HEK 293T/17 cells after 1 d (individual unmerged images are shown in Supporting Information Fig. S4†). Following uptake, the cells were allowed to grow continuously for 5 d and samples were imaged throughout. Approximately 3–4 d after the initial delivery, the QD signal began to separate from that of the endosomal marker, indicating endosomal escape in both cell lines. By day 5, the QDs had assumed a slightly more dispersed intracellular appearance that was completely distinct from that of the endosomes which had a more perinuclear localization. Longer incubation times did not improve on these results. Although the results were rather modest in terms of overall cellular labeling efficiency, it is clear that combining PULSin™ with mixed surface QDs could facilitate their endosomal escape. However, in addition to requiring several days to mediate endosomal escape of the QDs, PULSin™ also elicited a considerable degree of cytotoxicity in both cell lines (Fig. 5C and D). We found that the toxicity was attributable to the PULSin™ polymer alone. When cells were incubated with 100 nM mixed surface QDs alone, the viability of both COS-1 and HEK 293T/17 cells was approximately 80% while in the presence of either PULSin™ alone or QD-PULSin™ complexes, cell viability was reduced to less than 60%.

*Peptide-mediated delivery.* The use of peptides still remains the most popular means of facilitated QD delivery.<sup>10</sup> In this case, the QDs are decorated with a peptide that induces endocytosis by mediating interaction with specific cell surface receptors or more generally through electrostatic interactions with the cell surface.<sup>40</sup> For electrostatic interactions, peptides derived from the HIV-1 Tat protein remain the functional motif of choice as their high positive charge density interacts efficiently with negatively-charged cell surface receptors. These peptides deliver their cargo to endocytic vesicles although escape from these vesicles and subsequent localization to the cytoplasm and/or nucleus has been reported for several cargo materials including fluorophores, nucleic acids, proteins and even QDs (reviewed in ref. 41 and 42). As described earlier, our delivery of QDs with the polyarginine-containing CPP always resulted in their long-term sequestration within endolysosomal vesicles. Before testing other peptidyl sequences, we investigated whether Tat-based CPP delivery of QDs could be augmented by addition of endosmolytic agents to facilitate QD release from the endosomes to the cytosol.

Sucrose and chloroquine are two well known endosmolytic agents that have been shown to facilitate the release of endocytosed nucleic acids to the cytosol.<sup>43</sup> Sucrose accumulates within endocytic vesicles and promotes vesicle swelling and destabilization.<sup>44</sup> Chloroquine is an endolysosomal-tropic amine whose buffering capacity prevents endosomal acidification and slows down the rate of endocytosis, allowing more time for endosomal escape.<sup>45</sup> In our case, we self-assembled 510 nm DHLA-PEG QDs with CPP and incubated them with HEK 293T/17 cells for 2–3 h in the presence of increasing concentrations of either agent up to a maximum of 500 mM

sucrose or 500  $\mu$ M chloroquine. As shown in Supporting Information Fig. S5,† both compounds efficiently disrupted the endosomes at the highest concentrations as evidenced by the diffuse appearance of labeled transferrin in the cytosol. The QDs, however, remained punctate in appearance and were not well-dispersed despite the presence of the far more soluble PEGylated QD ligands.<sup>30</sup> We also noted significant cellular toxicity and morbidity, especially as the concentrations of each agent were increased (data not shown).

Nuclear localization signal (NLS) peptides bearing a sequence derived from the simian virus 40 T-antigen have been reported to mediate QD uptake and subsequent nuclear delivery in some cases.<sup>46</sup> Rozenzhak and co-workers utilized commercial Streptavidin functionalized QDs assembled with biotinylated NLS peptides and incubated with a secondary non-covalent peptide carrier (Pep-1) to create complexes for delivery to HeLa cells. They found a high degree of subsequent QD colocalization with the nuclear stain DAPI and little residual cytosolic or endosomal staining. Thus, in a conjugation approach similar to that used for the CPP, we assembled a histidine-tagged NLS peptide (see Experimental for sequence) onto the surface of QDs for delivery experiments. When incubated with HEK 293T/17 and COS-1 cells, however, the QDs were found to be completely internalized within endosomes, with no release to the cytosol or nuclear translocation observed even after culturing the cells for two days after QD uptake (data not shown).

Lastly, we tested the use of an amphiphilic peptide originally designed for the delivery of protein palmitoyl transferase 1 (PPT1) inhibitors across the blood-brain barrier.<sup>47,48</sup> This peptide, WG(Pal)VKIKKP<sub>9</sub>GGH<sub>6</sub> (referred to herein as Palm-1), consists of a core (Pal)VKIKK sequence where Pal is a palmitoyl group anchored to a synthetic diaminopropionic acid (Dap) residue. The VKIKK motif is derived from the sequence CVKIKK which is found at the C-terminus of the K-Ras protein and is thought to mediate electrostatic interactions with membranes.<sup>49</sup> In the K-Ras protein, the cysteine residue in CVKIKK is normally post-translationally modified with a palmitoyl group which inserts into the membrane allowing the protein to remain membrane-bound.<sup>50–52</sup> Similar to the other peptides tested above, the Palm-1 sequence was appended to a terminal His<sub>6</sub>-sequence to mediate self-assembly to the QD surface and this portion was separated from the core functional sequence by a poly(L-proline) (Pro)<sub>9</sub> sequence assumed to be in a helical structure and acting as a spacer.<sup>49</sup> COS-1 and HEK 293T/17 cells were incubated for 1–2 h with 550 nm DHLA PEG QD-Palm-1 complexes in the presence of AlexaFluor 647-transferrin. Imaging the cells at 1 h post delivery revealed that the QD complexes were internalized and adopted a punctate appearance that was completely colocalized within endosomes (data not shown). As shown in Fig. 6A and B, approximately 48 h post-delivery the QD signal separated from that of the endosomal marker in both cell lines and the QDs became well-dispersed, occupying the entire cell volume. Greater than 90% of cells observed were positive for initial QD uptake and of those, 77% showed a high degree of endosomal escape. Although a small degree of endosomal escape was observed at 24 h, QD release from endosomes was maximal at 48 h post-delivery and no



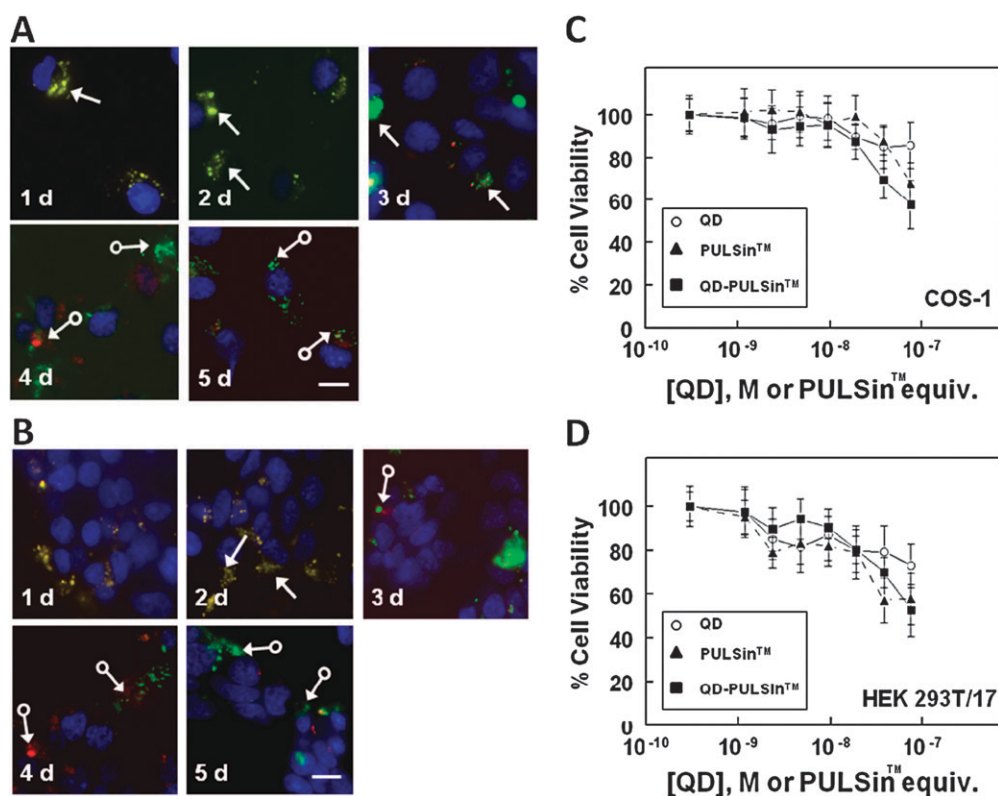


**Fig. 5** Cellular delivery and cytotoxicity of PULSin™-QD conjugates. 520 nm 1:1 DHLA:DHLA-PEG mixed surface QDs (100 nM final QD concentration) were complexed with PULSin™ polymer and incubated for 1–3 h with COS-1 cells (A) or HEK 293T/17 cells (B). Shown are images in which the DAPI, QD and AlexaFluor 647-transferrin images are merged at 1 d, 2 d, 3 d, 4 d and 5 d post-QD delivery. Regular arrows denote areas of colocalization between the QDs and endosomes (note yellow color of merged QD and transferrin signals). Open circle-terminated arrows indicate areas where the QD signal is separated from the endosomal marker. Scale bar is 10  $\mu$ m. Cytotoxicity data demonstrating the effects of the PULSin™-QD complexes on cellular proliferation are shown for COS-1 (C) and HEK 293T/17 cells (D). Cells were incubated with the complexes for 3 h, washed and subsequently cultured for 72 h prior to viability assay. When the QDs are present, the concentration given is that of the QDs. Each data point represents the mean  $\pm$  SD of triplicate measurements.

appreciable increase in escape efficiency was noted at 72 h or longer (data not shown). Some punctate areas of brighter QD fluorescence remained which were still colocalized with the transferrin, leading us to conclude that not all endosomal QDs were released with this peptide.

Importantly, we found that the QD-Palm-1 complexes elicited minimal concomitant cytotoxicity following uptake and endosomal escape, see Fig. 6C and D. In both COS-1 and HEK 293T/17 cells, at the QD-Palm-1 complex concentration required for efficient cytosolic delivery (100 nM), cell viability was greater than 85% even after 3 d. This value is quite close to the minimal cytotoxicity we also noted for delivering QD-CPP complexes to cells with short 1 h incubations in our previous study where the QDs remained sequestered within the endolysosomal system.<sup>13</sup> Thus, although the QDs are escaping from the endosomes with high efficiency, the finding of low concomitant cytotoxicity suggests that the integrity of the endolysosomal system is not being compromised in the process and adversely affecting metabolism or viability. With regards to the Palm-1 peptide itself, the specific mechanism by which it mediates cellular uptake and eventual endosomal escape is unclear. Our efforts are currently focused on trying to elucidate the role played by the different portions of the peptide to understand how endosomal

escape of these nanoparticle materials is mediated biologically. Such an understanding will be integral to improving the design and efficacy of these modular, multifunctional peptides. Another interesting finding from these data is the reduced cytotoxicity of the peptide-free QDs in HEK 293T/17 cells when their surface is capped exclusively with DHLA-PEG ligands (greater than 90% cell viability, Fig. 6D) compared to when a 1:1 surface of DHLA:DHLA-PEG ligand is used ( $\sim$ 75% cell viability, Fig. 5D). COS-1 cells, however, did not exhibit this differential cytotoxicity response to the two QD surfaces (Fig. 6C vs. 5C). This result not only demonstrates the important role played by the capping ligand in mediating QD biocompatibility but also points to inherent differences between the two cell lines.

## Conclusion

For QDs to reach their full potential in cellular applications, robust methods that allow their efficient delivery to the cytosol must be developed. In this study, we have built on and significantly expanded our previous findings that CPP-functionalized QDs can undergo endocytic uptake to cells.<sup>13</sup> We found that CPP-delivered QDs remain sequestered within endolysosomal compartments for up to three days in culture.

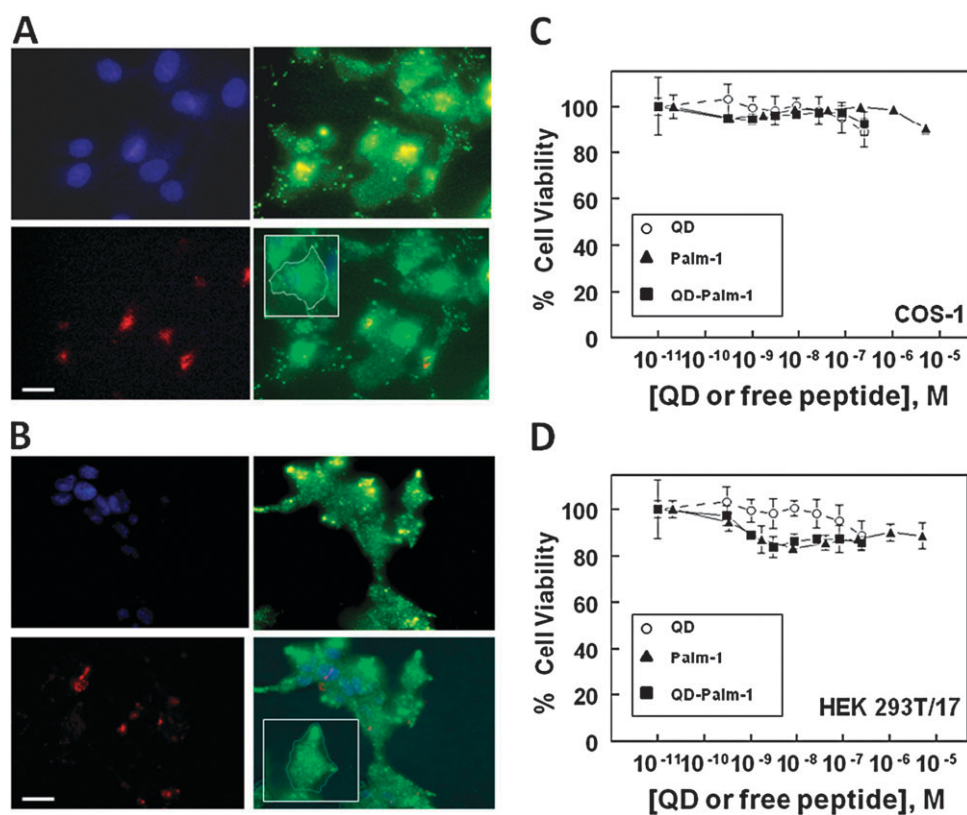


**Fig. 6** Cellular delivery and cytotoxicity of Palm-1 peptide-QD conjugates. 550 nm DHLA-PEG QDs were decorated with the Palm-1 peptide, incubated for 1–2 h along with AlexaFluor 647-transferrin, and imaged at 48 h post-delivery within COS-1 (A) or HEK 293T/17 cells (B). The QD signal is well-dispersed throughout the cell interior and is largely separated from the endosomal label in both cell lines. The inset in the merged images shows a single cell with the cell membrane highlighted for clarity. Panels C and D show corresponding cytotoxicity data for the inhibition of cellular proliferation by QD-Palm-1 complexes in COS-1 and HEK 293T/17 cells, respectively. Cells were incubated with the materials for 1 h, washed, and subsequently cultured for 72 h prior to viability assay. When the QDs are present, the concentration given is that of the QDs. Each data point represents the mean  $\pm$  SD of triplicate measurements.

We also demonstrated that the association of the CPP's terminal polyhistidine tract with the QD surface is of sufficient affinity to keep the QD–CPP complex intact throughout the culture period. The intracellular stability of the His–QD association over several days is notable, given the acidic environment of endolysosomal vesicles and has important implications for the development of intracellular sensors constructed using this self-assembly strategy. For example, as several protease sensors utilizing this strategy have been described<sup>53,54</sup> one envisioned application would be monitoring intracellular protease activity in real-time.

To address QD endosomal sequestration issues, we performed an extensive investigation of active delivery methods that bypass the endocytic pathway or facilitated delivery strategies that may provide a method for endosomal escape. We found that active methods such as electroporation and nucleofection result in the delivery of only modest amounts of aggregated QDs to the cytosol. The addition of common endosomal disrupting agents, including sucrose and chloroquine, to augment the QD–CPP complex during delivery did not achieve cytosolic delivery even at high concentrations. Similar results of efficient endocytic uptake with no concomitant cytosolic release were noted for most of the other polymers tested. We did, however, note that the commercial

PULSin™ polymer could mediate uptake and a modest endosomal escape of QDs to the cytosol, but at the cost of significant cytotoxicity which was traceable directly to the polymer itself. Lastly, we found that the Palm-1 peptide was able to mediate both rapid endocytosis and a subsequent efficient cytosolic delivery of QD conjugates 48 h after initial cell exposure. More importantly, the Palm-1 peptide appears to be well-tolerated metabolically, eliciting minimal cytotoxicity in the two cell lines tested. However, far more work is needed to understand its function for QD and other nanoparticle delivery beyond this initial observation.

A comparison of our results to others described in the literature also strongly suggests that the source of the QD materials and the nature of the QD surface ligand chemistry can be a significant determinant of the eventual intracellular fate of the nanoparticles. In many instances, the use of a similar peptide sequence or transfection reagent with a different QD material results in disparate outcomes. For example, polymer-encapsulated or commercial Streptavidin-functionalized QDs that have been used in some previous studies constitute rather large overall nanostructures (30–60 nm in diameter) yet they were still able to escape from endosomes.<sup>31,46</sup> Paradoxically, our smaller QD materials used here ( $\sim$ 8–10 nm in diameter)<sup>55</sup> when delivered with polymers

such as Lipofectamine 2000™ or PEI, remained entrapped within endocytic vesicles. These differences point to the need for a greater understanding of the influence of nanoparticle surface chemistry on uptake and intracellular fate and the need for the development of more robust methods to achieve cytosolic delivery, as exemplified by the Palm-1 results presented here. Success on these fronts will enable the implementation of the next generation of QD sensors capable of long-term intracellular monitoring.

## Experimental

### Materials

Sucrose, chloroquine, and polyethyleneimine (PEI, 25 kDa Mw, branched polymer) were purchased from Sigma (St. Louis, MO). Influx™ reagent, Lipofectamine2000™ and the subcellular organelle markers AlexaFluor 647-transferrin ( $\lambda_{\text{abs}}$  650 nm/ $\lambda_{\text{em}}$  668 nm), BODIPY TR-ceramide-BSA ( $\lambda_{\text{abs}}$  589 nm/ $\lambda_{\text{em}}$  616 nm), LysoTracker Red DND-99 ( $\lambda_{\text{abs}}$  577 nm/ $\lambda_{\text{em}}$  590 nm) and the nuclear stain DAPI ( $\lambda_{\text{abs}}$  350 nm/ $\lambda_{\text{em}}$  450 nm) were obtained from Invitrogen (Carlsbad, CA). PULSin™ was purchased from Polyplus-transfection (New York, NY). All other materials were obtained as described in the text.

### Quantum dots

CdSe–ZnS core–shell QDs with emission maxima centered at 510, 520, or 550 nm were synthesized and made hydrophilic by exchanging the native trioctylphosphine/trioctylphosphine oxide (TOP/TOPO) capping shell with either DHLA (dihydro-lipoic acid) or polyethylene glycol-(PEG) appended DHLA ligands as described previously, (see Fig. 1 for QD spectra and ligand structures).<sup>30,56</sup> These are subsequently referred to herein as DHLA or DHLA–PEG ligands. In general, PEGylated-QDs are preferred as they provide superior intracellular solubility and pH stability; however, some of the delivery reagents utilized required QDs with charged surfaces to mediate electrostatic interactions. 510 nm QDs capped with either DHLA or DHLA–PEG ligands were used for CPP-mediated delivery. The 520 nm QDs delivered by PULSin™, PEI or Lipofectamine2000™ were capped with a 1:1 ratiometric mix of DHLA and DHLA–PEG ligands. 550 nm QDs used for electroporation, nucleofection, Influx™- and peptide-mediated delivery were capped with DHLA–PEG.

### Peptides

The cell-penetrating peptide (CPP, R<sub>9</sub>GGLA(Aib)SGWKH<sub>6</sub>) used in this study is structurally similar to the CPP described previously.<sup>13</sup> It bears the same polyarginine tract (R<sub>9</sub>) used to mediate cellular uptake separated from a polyhistidine tract (H<sub>6</sub>) for assembly to the QD surface by a linker domain (GGLA(Aib)SGWK). Aib is the artificial residue alpha-amino isobutyric acid. The nuclear localization signal (NLS)-containing peptide was synthesized with the sequence H<sub>6</sub>WGLA(Aib)SGPKKKRKV. The palmitoylated peptide (Palm-1) sequence was WG(Pal)VKIKKP<sub>9</sub>GGH<sub>6</sub> where ‘Pal’ corresponds to a palmitate group that is covalently attached to a diaminopropionic acid functionality synthesized

into the peptide backbone. A nonspecific peptide with the sequence H<sub>6</sub>SLGAAAGSGC (essentially H<sub>6</sub>-spacer-cysteine) was labeled with Cy3-maleimide ( $\lambda_{\text{abs}}$  550 nm/ $\lambda_{\text{em}}$  570 nm, GE Healthcare, Piscataway NJ) on the terminal cysteine residue and used for FRET studies. All peptides were synthesized using Boc-solid phase peptide synthesis, purified by HPLC, and characterized by electrospray ionization mass spectrometry.<sup>13,57</sup> All peptide sequences are written in the conventional amino-to-carboxy terminus orientation.

### Cell culture

Human embryonic kidney (HEK 293T/17) and African green monkey kidney (COS-1) cell lines (ATCC, Manassas, VA) were used in the delivery experiments as they have been used in previous investigations of QD delivery and uptake.<sup>10,13</sup> The cells were cultured in complete growth medium (Dulbecco’s Modified Eagle’s Medium (DMEM; purchased from ATCC)) supplemented with 1% (v/v) antibiotic/antimycotic and 10% (v/v) heat inactivated fetal bovine serum (ATCC). Cells were cultured in T-25 flasks and incubated at 37 °C under 5% CO<sub>2</sub> atmosphere and a subculture was performed every 3–4 days as described.<sup>13</sup>

### Cellular delivery of quantum dots

All QD delivery experiments were performed on adherent cells seeded into the wells of Lab-Tek 8-well chambered #1 borosilicate coverglass (Nalge Nunc, Rochester, NY) coated with 2  $\mu\text{g mL}^{-1}$  fibronectin. For electroporation and nucleofection, adherent cells were harvested by trypsinization prior to performing QD delivery to cells in suspension. Cells were then seeded to chambered coverglass wells and imaged after cell attachment. The endosomal marker AlexaFluor 647-transferrin was included as indicated in the text. For imaging, cells were washed with phosphate buffered saline (PBS, 137 mM NaCl, 10 mM phosphate, 3 mM KCl, pH 7.4), fixed with 3.7% paraformaldehyde in PBS and nuclei were stained with DAPI (Sigma) unless otherwise indicated.

**Electroporation and nucleofection of QDs.** For electroporation, cells were harvested by trypsinization and recovered for 1 h in complete growth medium, pelleted, and resuspended in PBS. 510 nm DHLA–PEG QDs (0.5  $\mu\text{M}$  final concentration) were mixed with  $1 \times 10^4$  cells to a final volume of 100  $\mu\text{L}$  in PBS in a 0.2 mm electroporation cuvette. The cuvette was subjected to 100 V for a 20 ms pulse using a GenePulser XCell electroporator (Bio-Rad, Hercules, CA). Cells were resuspended in complete growth medium, seeded into fibronectin-coated 8-well chambered coverglass, fixed and imaged after 24 h. For nucleofection delivery,  $1 \times 10^6$  cells were harvested and resuspended in 100  $\mu\text{L}$  of Nucleofector™ reagent (Amaxa, Gaithersburg, MD). 510 nm DHLA–PEG QDs were included at a final concentration of 0.4  $\mu\text{M}$ . The cell/QD/reagent mixture was pulsed in the Nucleofector™ using a preset protocol adapted for each specific cell line.<sup>28,29</sup> Cells were cultured and imaged as described for electroporation. As a positive control, a plasmid encoding monomeric red fluorescent protein (RFP) was delivered using the same conditions as those for QD delivery and positive expression of the RFP confirmed.

**Influx™-mediated delivery.** The Influx™ cell-loading reagent mediates the intracellular release of materials internalized *via* pinocytic vesicles by delivering the materials to cells in a hypertonic medium followed by the transfer of the cells to a hypotonic medium to induce vesicle disruption.<sup>58</sup> 510 nm DHLA-PEG QDs were diluted to a final concentration of 300–800 nM in the supplied hypertonic delivery media according to manufacturer's instructions and incubated on the cells for 30 min at 37 °C. The hypertonic medium was exchanged for hypotonic medium (serum-free culture medium diluted by 40% with deionized water) and incubated on the cells for 3 min. The cells were then recovered in complete growth medium for 30 min and cultured for various lengths of time prior to washing and fixation for imaging.

**Lipofectamine 2000™-mediated delivery.** 520 nm QDs with a 1:1 mixed surface of DHLA:DHLA-PEG were incubated with Lipofectamine 2000™ for 20 min in serum free medium at a ratio of 1 µL Lipofectamine 2000™ per 1.5 pmol QD. The complexes, at a final QD concentration of 75 nM, were incubated with the cells for 4 h, removed and replaced with complete growth medium. The cells were then cultured for 24–36 h prior to washing and fixation.

**Polyethyleneimine-mediated delivery.** PEI was incubated with 520 nm mixed surface DHLA:DHLA-PEG QDs in serum free medium at a ratio of 10 µg PEI per 1 pmol QD for 15 min. This ratio was previously determined in delivery experiments to yield maximal QD uptake. The complexes were then diluted into serum free media to a final QD concentration of 75–100 nM, incubated with cells for 2 h and removed. Cells were then cultured in complete media for 24–36 h, washed and fixed.

**PULSin™-mediated delivery.** A stock solution of 520 nm DHLA:DHLA-PEG QDs (1 µM in 0.1 M borate buffer, pH 8.9) was diluted to 0.5 µM in HEPES (4-(2-hydroxyethyl)-1-piperazineethanesulfonic acid, pH 8.2). PULSin™ delivery reagent was added (1 µL per 20 pmol QD) and complex formation occurred for 20 min at 25 °C. The complexes were diluted into serum free medium to a final QD concentration of 100 nM and incubated on cells for 1–3 h after which complexes were removed and replaced with complete growth medium. Cells were subsequently cultured for up to 5 days to monitor intracellular QD distribution.

**Peptide-mediated delivery.** QD-CPP, QD-NLS and QD-Palm-1 bioconjugates were formed by diluting a stock solution of preformed peptide-QD complexes (1 µM QD assembled with 25 CPP, 30 NLS or 75 Palm-1 peptides per QD in 0.1 M borate buffer, pH 8.9) into complete growth medium to a final QD concentration of 50–100 nM. These peptide:QD ratios were determined experimentally for each peptide to be that ratio that yielded the optimal degree of cell uptake. The self-assembled bioconjugates were then incubated with cells as described in the text. For monitoring the intracellular fate of QD-CPP assemblies, AlexaFluor 647-transferrin, LysoTracker Red DND-99 and BODIPY TR-ceramide-BSA subcellular markers were included at the manufacturer's recommended concentrations. In some experiments, QD-CPP

complexes were also incubated with cells in the presence of pyrenebutyrate (100 µM), sucrose (500 mM) or chloroquine (500 µM) to test either membrane translocation or to induce endosomal disruption and release of the internalized QDs to the cytosol. The general scheme for the assembly of QDs with cationic polymers, cationic amphiphiles or histidine-tagged peptides is shown in Fig. 1B.

### Microscopy and image analysis

The intracellular distribution of QDs was analyzed by differential interference contrast (DIC) and epifluorescence microscopy using an Olympus IX-71 total internal reflection fluorescence microscope equipped with a 60x oil immersion lens. Samples were excited using a Xe lamp and images were collected using standard filter sets for DAPI, FITC (for QDs), TRITC (for Cy3 and Texas Red) and Cy5 (for AF647-transferrin). Merged images were generated using Adobe PhotoShop. Förster resonance energy transfer (FRET) measurements for determining the intracellular stability of QD-peptide association over time were performed by imaging 510 nm donor QD-CPP conjugates decorated with approximately 2 Cy3-labeled acceptor peptides per QD. The Förster radius ( $R_0$ ) for this donor-acceptor pair is approximately 47 Å. Side-by-side split fluorescence images were collected and quantitated using a DualView system (Optical Insights, Tucson, AZ) equipped with a 565 nm dichroic filter. The QDs and Cy3 were excited at 488 nm and their respective emissions were separated with the dichroic filter and deconvoluted. Signal intensities were measured at various time points over a three day period to calculate the Cy3/QD emission ratio (defined as  $[Cy3_{em}/Cy3_{em} + QD_{em}]$ ). This ratio corrects for any direct excitation of the Cy3 dye which may occur intracellularly.<sup>26</sup> To correct for any leakage of the QD signal into the Cy3 channel, this ratio was also calculated for cells exposed to QD-CPP alone (no Cy3-labeled peptide) and subtracted from the Cy3/QD emission ratio to give the corrected ratio ( $[Cy3_{em}/Cy3_{em} + QD_{em}] - QD_{em}$ ). A decrease in this ratio over time indicates either the dissociation of the Cy3-labeled peptide from the QD surface or degradation of the Cy3 fluorophore.

### Cytotoxicity assays

Cellular toxicity was assessed using the CellTiter 96 Cell Proliferation Assay (Promega, Madison WI) according to the manufacturer's instructions. This assay is based upon the conversion of a tetrazolium substrate to a formazan product by viable cells at the assay end point.<sup>59</sup> Cells ( $1 \times 10^4$  cells/well) were cultured in 96-well microtiter plates in complete growth medium in the presence of increasing concentrations of QDs, free peptide or polymer, or QDs in complex with peptide or polymer. In each case, the materials were incubated with the cells for the time required for efficient QD uptake. The materials were subsequently replaced with complete growth medium and the cells were cultured for 72 h.

### Acknowledgements

The authors acknowledge DTRA, NRL Nanosciences Institute and ONR for support. C.E.B. and D.F. were

supported by an NRC fellowship. K.B. acknowledges an ASEE fellowship. The authors also gratefully acknowledge Dr Thomas Pons for assistance with the intracellular FRET analysis.

## References

- 1 Y.-P. Chang, F. Pinaud, J. Antelman and S. Weiss, *J. Biophotonics*, 2008, **1**, 287–298.
- 2 P. Juzenas, W. Chen, Y.-P. Sun, M. A. N. Coelho, R. Generalov, N. Generalova and I. L. Christensen, *Adv. Drug Delivery Rev.*, 2008, **60**, 1600–1614.
- 3 W. A. Hild, M. Breunig and A. Goepferich, *Eur. J. Pharm. Biopharm.*, 2008, **68**, 153–168.
- 4 W. Parak, T. Pellegrino and C. Plank, *Nanotechnology*, 2005, **16**, R9–R25.
- 5 A. P. Alivisatos, W. Gu and C. A. Larabell, *Annu. Rev. Biomed. Eng.*, 2005, **7**, 55–76.
- 6 J. K. Jaiswal, H. Mattoussi, J. M. Mauro and S. M. Simon, *Nat. Biotechnol.*, 2003, **21**, 47–51.
- 7 P. Alivisatos, *Nat. Biotechnol.*, 2004, **22**, 47–52.
- 8 I. Medintz, H. Uyeda, E. Goldman and H. Mattoussi, *Nat. Mater.*, 2005, **4**, 435–446.
- 9 W. J. Parak, D. Gerion, T. Pellegrino, D. Zanchet, C. Micheel, S. C. Williams, R. Boudreau, M. A. Le Gros, C. A. Larabell and A. P. Alivisatos, *Nanotechnology*, 2003, **14**, R15–R27.
- 10 J. B. Delehanty, H. Mattoussi and I. L. Medintz, *Anal. Bioanal. Chem.*, 2009, **393**, 1091–1105.
- 11 C. K. Payne, S. A. Jones, C. Chen and X. Zhuang, *Traffic*, 2007, **8**, 389–401.
- 12 G. Ruan, A. Agrawal, A. I. Marcus and S. Nie, *J. Am. Chem. Soc.*, 2007, **129**, 14759–14766.
- 13 J. B. Delehanty, I. L. Medintz, T. Pons, F. M. Brunel, P. E. Dawson and H. Mattoussi, *Bioconjugate Chem.*, 2006, **17**, 920–927.
- 14 K. E. Sapsford, T. Pons, I. L. Medintz, S. Higashiya, F. M. Brunel, P. E. Dawson and H. Mattoussi, *J. Phys. Chem. C*, 2007, **111**, 11528–11538.
- 15 E. Vivès, J. Schmidt and A. Pèlerin, *Biochim. Biophys. Acta, Rev. Cancer*, 2008, **1786**, 126–138.
- 16 I. L. Medintz, T. Pons, J. B. Delehanty, K. Susumu, F. M. Brunel, P. E. Dawson and H. Mattoussi, *Bioconjugate Chem.*, 2008, **19**, 1785–1795.
- 17 J. F. Presley, S. Mayor, K. W. Dunn, L. S. Johnson, T. E. McGraw and F. R. Maxfield, *J. Cell Biol.*, 1993, **122**, 1231–1241.
- 18 J. S. Herskovits, C. C. Burgess, R. A. Obar and R. B. Vallee, *J. Cell Biol.*, 1993, **122**, 565–578.
- 19 T. Harder and V. Gerke, *J. Cell Biol.*, 1993, **123**, 1119–1132.
- 20 R. E. Pagano, O. C. Martin, H. C. Kang and R. P. Haugland, *J. Cell Biol.*, 1991, **113**, 1267–1279.
- 21 C. Tekle, B. Deurs, K. Sandvig and T. G. Iversen, *Nano Lett.*, 2008, **8**, 1858–1865.
- 22 D. J. Bharali, D. W. Lucey, H. Jayakumar, H. E. Pudavar and P. N. Prasad, *J. Am. Chem. Soc.*, 2005, **127**, 11364–11371.
- 23 J. Qian, K. T. Yong, I. Roy, T. Y. Ohulchanskyy, E. J. Bergey, H. H. Lee, K. M. Tramosch, S. He, A. Maitra and P. N. Prasad, *J. Phys. Chem. B*, 2007, **111**, 6969–6972.
- 24 S. Kornfeld and I. Mellman, *Ann. Review Cell Bio.*, 1989, **5**, 483–525.
- 25 K. Honey and A. Y. Rudensky, *Nature Reviews*, 2003, **3**, 472–482.
- 26 A. R. Clapp, T. Pons, I. L. Medintz, J. B. Delehanty, J. S. Melinger, T. Tiefenbrunn, P. E. Dawson, B. R. Fisher, B. O'Rourke and H. Mattoussi, *Adv. Mater.*, 2007, **19**, 1921–1926.
- 27 E. Neumann, M. Schaefer-Ridder, Y. Wang and P. H. Hofschneider, *The EMBO Journal*, 1982, **1**, 841–845.
- 28 S. Marchenko and L. Flanagan, *J. Vis. Exp.*, 2007, 240.
- 29 N. Iversen, B. Birkenes, K. Torsdalen and S. Djurovic, *Genetic Vaccines and Therapy*, 2005, **3**, 2.
- 30 B. C. Mei, K. Susumu, I. L. Medintz, J. B. Delehanty, T. J. Mountziaris and H. Mattoussi, *J. Mater. Chem.*, 2008, **18**, 4949–4958.
- 31 A. M. Derfus, W. C. W. Chan and S. N. Bhatia, *Adv. Mater.*, 2004, **16**, 961–966.
- 32 F. Q. Chen and D. Gerion, *Nano Lett.*, 2004, **4**, 1827–1832.
- 33 S. D. Conner and S. L. Schmid, *Nature*, 2003, **422**, 37–44.
- 34 B. J. Nichols and J. Lippincott-Schwartz, *Trends Cell Biol.*, 2001, **11**, 406–412.
- 35 M. Neu, D. Fischer and T. Kissel, *J. Gene Med.*, 2005, **7**, 992–1009.
- 36 D. Hoekstra, J. Rejman, L. Wasungu, F. Shi and I. Zuhorn, *Biochem. Soc. Trans.*, 2007, **35**, 68–71.
- 37 H. T. Uyeda, I. L. Medintz, J. K. Jaiswal, S. M. Simon and H. Mattoussi, *J. Am. Chem. Soc.*, 2005, **127**, 3870–3878.
- 38 H. Duan and S. Nie, *J. Am. Chem. Soc.*, 2007, **129**, 3333–3338.
- 39 A. E. Jablonski, W. H. Humphries and C. K. Payne, *J. Phys. Chem. B*, 2009, **113**, 405–408.
- 40 S. El-Andaloussi, T. Holm and U. Langel, *Curr. Pharm. Des.*, 2005, **11**, 3597–3611.
- 41 K. Melikov and L. V. Chernomordik, *Cell. Mol. Life Sci.*, 2005, **62**, 2739–2749.
- 42 M. Zhao and R. Weissleder, *Med. Res. Rev.*, 2004, **24**, 1–12.
- 43 S. Abes, D. Williams, P. Prevot, A. Thierry, M. J. Gait and B. Lebleu, *J. Controlled Release*, 2006, **110**, 595–604.
- 44 T. Kato, S. Okada, T. Yutaka and H. Yabuuchi, *Mol. Cell. Biochemistry*, 1984, **60**, 83–98.
- 45 V. Ferrari and D. J. Cutler, *Biochem. Pharmacol.*, 1991, **41**, 23–30.
- 46 S. M. Rozenzhak, M. P. Kadakia, T. M. Caserta, T. R. Westbrook, M. O. Stone and R. R. Naik, *Chem. Commun.*, 2005, 2217–2219.
- 47 S. Cho, P. E. Dawson and G. Dawson, *J. Neurosci. Res.*, 2000, **62**, 234–240.
- 48 G. Dawson, S. A. Dawson, C. Marinzi and P. E. Dawson, *Cancer Lett.*, 2002, **187**, 163–168.
- 49 J. P. McGrath, D. J. Capon, D. H. Smith, E. Y. Chen, P. H. Seeburg, D. V. Goeddel and A. D. Levinson, *Nature*, 1983, **304**, 501–506.
- 50 M. D. Resh, *Cell. Signalling*, 1996, **8**, 403–412.
- 51 M. D. Resh, *Biochim. Biophys. Acta, Mol. Cell Res.*, 1999, **1451**, 1–16.
- 52 J. T. Dunphy and M. E. Linder, *Biochim. Biophys. Acta, Mol. Cell Biol. Lipids*, 1998, **1436**, 245–261.
- 53 I. L. Medintz, A. R. Clapp, F. M. Brunel, T. Tiefenbrunn, H. T. Uyeda, E. L. Chang, J. R. Deschamps, P. E. Dawson and H. Mattoussi, *Nat. Mater.*, 2006, **5**, 581–589.
- 54 K. Boeneman, B. C. Mei, A. M. Dennis, G. Bao, J. R. Deschamps, H. Mattoussi and I. L. Medintz, *J. Am. Chem. Soc.*, 2009, **131**, 3828–3829.
- 55 T. Pons, H. T. Uyeda, I. L. Medintz and H. Mattoussi, *J. Phys. Chem. B*, 2006, **110**, 20308–20316.
- 56 H. Mattoussi, J. M. Mauro, E. R. Goldman, G. P. Anderson, V. C. Sundar, F. V. Mikulec and M. G. Bawendi, *J. Am. Chem. Soc.*, 2000, **122**, 12142–12150.
- 57 M. Schnolzer, P. Alewood, A. Jones, D. Alewood and S. B. Kent, *Int. J. Pept. Protein Res.*, 1992, **40**, 180–193.
- 58 A. Quintana and M. Hoth, *Cell Calcium*, 2004, **36**, 99–109.
- 59 T. Mosmann, *J. Immunol. Methods*, 1983, **65**, 55–63.